International Journal of Hydrological and Environmental for Sustainability
Volume 5, Issue 2, 75-100.
e_ISSN: 2828-5050
https://www.journal.foundae.com/index.php/ijhes

Oil Palm Empty Fruit Bunch-Derived Cellulose Acetate-Zeolite Mixed Matrix Membrane Adsorbers (MMMAs) for Ammonia Removal in Palm Oil Mill Effluent Wastewater Treatment

Cut Riski
Department of Chemistry,
Faculty of Mathematics and Natural Sciences,
Universitas Syiah Kuala,
INDONESIA

Julinawati
Department of Chemistry,
Faculty of Mathematics and Natural Sciences,
Universitas Syiah Kuala,
INDONESIA

Mutia Farida
Department of Chemistry,
Faculty of Mathematics and Natural Sciences,
Universitas Syiah Kuala,
INDONESIA

Mohd Rashidi Abdull Manap
Department of Chemistry,
Faculty of Science,
Universiti Putra Malaysia,
MALAYSIA

Saiful*
[1]Department of Chemistry,
Faculty of Mathematics and Natural Sciences,
Universitas Syiah Kuala,
[2]Oil Palm and Coconut Research Center,
Universitas Syiah Kuala,
[3]Research Center for Environmental and Natural Resources, Universitas Syiah Kuala,
INDONESIA

***Correspondence: E-mail:** saiful@usk.ac.id

Article Info

Article history:

Received: January 19, 2026
Revised: May 31, 2026
Accepted: June 08, 2026

Abstract

This study developed cellulose acetate-zeolite mixed matrix membrane adsorbers (CA-zeolite MMMAs) using cellulose acetate synthesized from OPEFB as the polymer matrix and natural mordenite zeolite as the adsorptive inorganic filler. The membranes were fabricated to enhance ammonia-nitrogen removal from synthetic ammonia solution and palm oil mill effluent (POME). Zeolite incorporation improved several membrane properties, including pure water flux, swelling degree, and porosity, compared with pristine cellulose acetate membranes. However, tensile strength and elongation decreased after zeolite addition, indicating a trade-off between adsorption-related properties and mechanical flexibility. The optimum adsorption performance was achieved using the CA-zeolite MMMA with 30% zeolite loading and a contact time of 70 min, producing an ammonia adsorption capacity of 1.051 mg/g under the selected operating conditions. Adsorption kinetic analysis showed that the pseudo-second-order model provided a better fit than the pseudo-first-order model, with an R^2 value of 0.9104. The adsorption equilibrium was better represented by the Langmuir isotherm model, with an R^2 value of 0.9247. The optimized membrane also showed regeneration potential, with first-cycle regeneration efficiencies of 83.37% using NaCl and 73.52% using HCl. When applied to actual POME, the membrane reduced ammonia concentration from 173.93 mg/L to 50.161 mg/L in batch adsorption and 52.136 mg/L in filtration, corresponding to removal efficiencies of 71.16% and 70.02%, respectively. Although the treated effluent remained above the regulatory discharge limit of 20 mg/L, the results demonstrate that OPEFB-derived CA-zeolite MMMAs have potential as pretreatment or polishing materials for ammonia-nitrogen removal from POME.

Keywords: oil palm empty fruit bunch, cellulose acetate, natural zeolite, mixed matrix membrane adsorber, ammonia-nitrogen removal, palm oil mill effluent

To cite this article: Riski, C., Julinawati, Farida, M., Manap, M. R. A., and Saiful. (2026). Oil Palm Empty Fruit Bunch-Derived Cellulose Acetate-Zeolite Mixed Matrix Membrane Adsorbers (MMMAs) for Ammonia Removal in Palm Oil Mill Effluent Wastewater Treatment. *International Journal of Hydrological and Environmental for Sustainability, 5*(2), 75-100. https://doi.org/10.58524/ijhes.v5i2.1267

INTRODUCTION

The palm oil industry constitutes a critical sector in the economies of many countries, including Indonesia. Its primary product, crude palm oil (CPO), is widely utilized across various industries, ranging from food to cosmetics. Despite its economic importance, the industry faces significant challenges in managing both liquid and solid waste streams generated during production. Wastewater from palm oil mills or palm oil mill effluent (POME) contains hazardous substances, such as oil, grease, and ammonia, which may cause severe environmental pollution if inadequately treated. In addition to POME, oil palm empty fruit bunches (OPEFB) are generated in large quantities as lignocellulosic solid residues. Although often underutilized, OPEFB contains cellulose that can be converted into cellulose acetate, thereby supporting biomass valorization and circular-economy-oriented wastewater treatment materials.

The disposal of industrial and agricultural waste has substantial social, economic, and environmental implications. A major nitrogenous pollutant in palm oil mill effluent (POME) is ammoniacal nitrogen, which may exist as unionized ammonia (NH_3) and ionized ammonium (NH_4^+), depending on pH and temperature. These species are toxic to aquatic organisms and contribute to eutrophication when discharged into water bodies without proper treatment. Eutrophication can lead to excessive algal growth, depletion of dissolved oxygen, and ultimately the mortality of aquatic organisms. Ammonia, in both its molecular (NH_3) and ionic (NH_4^+) forms, exhibits high toxicity even at low concentrations and poses serious risks to aquatic ecosystems and human health (Rohani et al., 2021). Therefore, reducing ammonia or ammoniacal nitrogen concentration before discharge is essential to meet environmental quality requirements and protect receiving water bodies.

The palm oil milling industry represents a significant source of ammonia-containing wastewater. Indonesia has 34 palm oil industrial companies registered with the Ministry of Industry and distributed nationwide. In Aceh Province alone, there are 55 palm oil mills, with plantation areas ranging from approximately 200,000 to 400,000 hectares. The expansion of palm oil processing facilities has resulted in increased crude palm oil (CPO) production (Wibowo et al., 2018), accompanied by a substantial rise in by-product waste, particularly in the form of palm oil mill effluent (POME). Under the Indonesian wastewater discharge regulation, the allowable ammonia concentration for discharge is 20 mg/L; therefore, POME with ammonia concentrations exceeding this limit requires further treatment before being released into the environment (Ministry of Environment of the Republic of Indonesia, 2014).

Conventional ammonia removal methods typically involve pond systems, including biological ponds and lagoons. However, these approaches present several limitations, such as large land requirements, long hydraulic retention times, inconsistent nutrient removal performance, possible odor generation, and the need for additional treatment or stabilization before the effluent can meet regulatory discharge standards (Ministry of Environment of the Republic of Indonesia, 2014). Membrane technology has emerged as a promising alternative due to its high efficiency in contaminant separation and removal. Nevertheless, challenges related to membrane stability, fouling resistance, and performance under varying operational conditions persist. Consequently, integrated approaches, such as Mixed Matrix Membrane Adsorbers (MMMAs), have been proposed. MMMAs combine membrane separation with adsorption, thereby enabling contaminant removal through both physical retention and interaction with active adsorptive sites. This approach may offer shorter processing times and more compact treatment units compared with conventional pond-based systems, thereby contributing to improved water resource management.

Mixed Matrix Membrane Adsorbers (MMMAs) represent an advancement in membrane technology through the integration of organic and inorganic materials to enhance performance. In this study, cellulose acetate was selected as the organic matrix due to its biodegradability and environmental compatibility, while zeolite was employed as an inorganic filler owing to its ion-exchange properties and affinity toward ammonium species. This combination is expected to yield membranes with enhanced performance for ammonia removal from palm oil mill effluent. MMMAs offer several advantages, including relatively simple preparation, high filler selectivity, and the potential to improve selected physicochemical properties, such as porosity, hydrophilicity, permeability, and adsorption capacity (Qadir et al., 2017). Furthermore, they are reusable and amenable to scale-up, as they integrate adsorption and filtration processes within a single system.

However, the incorporation of inorganic particles may also affect membrane mechanical strength, particle dispersion, and structural integrity; therefore, these properties must be carefully evaluated.

Based on these considerations, this study focuses on the fabrication of composite membranes (MMMAs) using cellulose acetate synthesized from oil palm empty fruit bunches as the membrane matrix, optimized through the incorporation of natural mordenite zeolite particles as fillers. Previous research by Sanaeepur et al. (2015) developed zeolite Y/cellulose acetate MMMAs via an ion-exchange process; however, their study focused on CO_2/N_2 separation. In contrast, the present study investigates the application of natural zeolite and cellulose acetate membranes derived from oil palm empty fruit bunch fibers for ammonia adsorption in wastewater. Unlike previous cellulose acetate-zeolite mixed matrix membrane studies that mainly focused on gas separation or general water filtration, this study develops OPEFB-derived cellulose acetate-natural mordenite zeolite MMMAs specifically for ammonia removal from actual POME. The fabricated membranes were subsequently characterized and applied to reduce ammonia or ammoniacal nitrogen concentrations in palm oil mill effluent.

Therefore, this study aims to synthesize cellulose acetate from OPEFB, activate natural mordenite zeolite, fabricate cellulose acetate-zeolite MMMAs with different zeolite loadings, characterize their physicochemical, morphological, permeability, and mechanical properties, evaluate ammonia adsorption performance under different operating conditions, analyze adsorption kinetics and isotherms, assess membrane regeneration potential, and test the optimum membrane using actual POME.

METHOD

The research was conducted at the Physical Chemistry Laboratory, Department of Chemistry, Faculty of Mathematics and Natural Sciences, Universitas Syiah Kuala, Darussalam, Banda Aceh, from February to August 2024. Fourier Transform Infrared (FT-IR) analysis was performed at the Analysis and Instrumentation Laboratory, Faculty of Mathematics and Natural Sciences, Universitas Syiah Kuala. Scanning Electron Microscopy–Energy Dispersive X-ray (SEM-EDX) and X-ray Diffraction (XRD) analyses were carried out at the Chemistry Laboratory, Institut Teknologi Bandung (ITB), Indonesia.

Equipment/ Materials/Reagents

The equipment used in this study included standard laboratory glassware (Pyrex or Duran), glass plates, an oven (Memmert), an analytical balance, graduated cylinders, volumetric flasks, Erlenmeyer flasks, volumetric pipettes, dropper pipettes, pipette fillers, sample bottles, a hot plate, a magnetic stirrer, a Soxhlet apparatus, a reflux system, a pH meter, a digital micrometer, a blender, aluminum foil, a ball mill, a stainless-steel hammer, a shaker, scissors, a sonicator, a centrifuge, and a UV–Vis spectrophotometer. Instrumental analyses were conducted using FT-IR, XRD, and SEM-EDX instruments. A casting applicator or casting knife was used to control membrane casting thickness during membrane preparation.

The primary raw materials used in this study were oil palm empty fruit bunches obtained from PT Beurata Subur Persada (Nagan Raya) and natural zeolite sourced from Klaten, Central Java. Palm oil mill effluent (POME) samples were collected from the fourth (aerobic) pond of PT Socfindo, Nagan Raya Regency. The chemicals used in this study included ethanol (C_2H_5OH), sodium hydroxide (NaOH), hydrochloric acid (HCl), sodium hypochlorite (NaOCl), formic acid (CH_2O_2), sulfuric acid (H_2SO_4), glacial acetic acid, acetic anhydride, ammonium chloride (NH_4Cl) as the ammonia-nitrogen standard, distilled water (H_2O), sodium chloride (NaCl), acetone (C_3H_6O), and dimethylformamide (DMF).

Experiment

Isolation of Cellulose from Oil Palm Empty Fruit Bunches

Oil palm empty fruit bunches (OPEFB) were used as the raw material for cellulose isolation, following the method reported by Saiful et al. (2024). The OPEFB fibers were initially washed with a 1% detergent solution and rinsed with distilled water until the rinse water became colorless. The fibers were then dried and cut into small pieces. Subsequently, the fibers were subjected to Soxhlet

extraction using 200 mL of 70% (v/v) ethanol for 6 hours. The extracted fibers were washed with distilled water to remove residual ethanol and then dried. A total of 10 g of the treated fibers was suspended in a mixture of 100 mL of 10% NaOH and 100 mL of 10% NaOCl. The suspension was covered with aluminum foil and autoclaved at 121°C for 1 hour. The fibers were subsequently rinsed repeatedly until the washing water became colorless. In the next step, the fibers were immersed in a solution containing 20% formic acid and 10% NaOCl and heated in a water bath at 85°C for 2 hours. The fibers were then washed with 10% formic acid, followed by rinsing with distilled water, yielding light yellow cellulose. To obtain purified cellulose, the material was further treated with a mixture of 10% NaOCl and 10% NaOH at 60°C for 90 minutes. The resulting white cellulose was then collected and dried to constant weight before further use.

Synthesis of Cellulose Acetate

Cellulose acetate was synthesized according to Saiful et al. (2024), beginning with an activation step. A total of 10 g of isolated cellulose was reacted with 250 mL of glacial acetic acid and stirred at 38°C for 3 hours. The acetylation step was then carried out by adding 75 mL of acetic anhydride and 0.5 mL of sulfuric acid as a catalyst, followed by stirring at 30°C for 2.5 hours until a homogeneous yellowish-brown solution was obtained. Subsequently, 25 mL of distilled water and 50 mL of glacial acetic acid were added, and the mixture was stirred for an additional 30 minutes. The hydrolysis step was performed by adding 2 g of sodium acetate and stirring for 5 minutes. The resulting solution was diluted with distilled water at a ratio of 1:2 and vigorously shaken until a white precipitate formed. The precipitate was filtered, washed with distilled water until the acetic acid odor was no longer detectable, and dried in an oven at 30°C for 24 hours or until constant mass was reached. The final product, obtained as a white powder, was characterized using FT-IR to confirm the formation of cellulose acetate.

The cellulose acetate yield was calculated based on the dry mass of cellulose acetate obtained relative to the initial dry mass of cellulose. Because acetylation introduces acetyl groups into the cellulose structure, the product mass may exceed the initial cellulose mass; therefore, a yield above 100% was interpreted with consideration of acetyl-group substitution and possible mass gain during derivatization. The degree of substitution or acetyl content was not determined in this study; therefore, FT-IR analysis was used as qualitative evidence for successful acetylation. This limitation is acknowledged because degree of substitution and acetyl content provide quantitative information on cellulose acetate quality.

Activation of Natural Zeolite

Natural zeolite obtained from Klaten, Central Java, was sieved using a 100-mesh sieve prior to activation, corresponding to a particle size of approximately less than 149 micrometers. The activation process was conducted by treating the zeolite with 6% HCl at a solid-to-liquid ratio of 1:10 under magnetic stirring for 3 hours. The treated zeolite was then filtered and washed repeatedly with distilled water until neutral pH was achieved. The washed zeolite was dried at 110°C for 2 hours and subsequently calcined at 500°C for 3 hours. The activated zeolite was characterized using SEM-EDX and XRD to confirm successful activation and to identify its crystalline structure. BET surface area, pore volume, and cation exchange capacity were not measured in this study; therefore, the interpretation of adsorption performance was based on XRD, SEM-EDX, and adsorption data.

Fabrication of Cellulose Acetate–Zeolite MMMAs

The fabrication of cellulose acetate–zeolite mixed matrix membrane adsorbers (MMMAs) followed the method reported by Saiful et al. (2024) with modifications. Membranes were prepared using the phase inversion method. The dope solution consisted of 11 wt% cellulose acetate, 69 wt% acetone, and 20 wt% dimethylformamide (DMF). The mixture was stirred for approximately 15 hours until a homogeneous solution was obtained. Zeolite was incorporated into the polymer solution at different loading levels (0, 10, 20, and 30 wt%) to impart adsorption properties. Prior to casting, the zeolite-containing dope solution was dispersed by stirring and sonication for [insert

actual sonication duration] to improve particle distribution in the polymer matrix. The resulting mixture was cast onto a glass plate using a casting thickness of [insert actual casting gap/thickness] and was immersed in the coagulation bath after an evaporation time of 0 min because the cast film was immediately immersed after casting. The coagulation bath contained distilled water at [insert actual coagulation bath temperature]°C, followed by washing with running water to remove residual solvents. The membranes were stored [insert wet/dry storage condition] before characterization and adsorption testing. Final membrane thickness was measured using a digital micrometer and should be reported for each formulation. The zeolite loading percentage was calculated using the following equation:

$$\text{Loading (\%)} = \frac{Wzeolite}{Wzeolite + Wcellulose\ acetate} \text{ x } 100\% \qquad (1)$$

Table 1. Composition of MMMAs with varying zeolite loading.

Zeolite Loading (%)	Cellulose Acetate (g)	Zeolite (g)
0	2,75	0
10	2,75	0,305
20	2,75	0,687
30	2,75	1,178

Characterization was performed on both pristine cellulose acetate membranes and cellulose acetate–zeolite MMMAs. The analyses included Fourier Transform Infrared (FT-IR), Scanning Electron Microscopy–Energy Dispersive X-ray (SEM-EDX), X-ray Diffraction (XRD), flux measurement, tensile strength testing, swelling degree determination, and porosity analysis. Membrane thickness was measured at [insert number] different positions, and the average value was used for membrane property evaluation. Possible zeolite agglomeration at high filler loading was evaluated from SEM images.

Analysis of Ammonia in the Filtrate Using a UV–Vis Spectrophotometry Preparation of Nessler Reagent

Nessler reagent was prepared by dissolving 50 g of potassium iodide (KI) in 50 mL of cold distilled water. A saturated mercury(II) chloride ($HgCl_2$) solution was prepared separately by dissolving approximately 22 g of $HgCl_2$ in 350 mL of distilled water. The $HgCl_2$ solution was then added dropwise to the KI solution until a precipitate formed. Subsequently, 500 mL of 5 M sodium hydroxide (NaOH) was added, and the solution was diluted to a final volume of 1 L with distilled water. The mixture was filtered, and the clear filtrate was stored in a dark bottle.

Preparation of Standard Solutions

A 1000 mg/L ammonia-nitrogen (NH_3-N) stock solution was prepared by dissolving 3.819 g of ammonium chloride (NH_4Cl), previously dried at 100°C for 2 hours, in distilled water and diluting to 1000 mL in a volumetric flask (Nurman et al., 2022). A 10 mg/L NH_3-N working solution was then prepared by pipetting 10 mL of the stock solution into a 1000 mL volumetric flask and diluting to volume with distilled water.

Determination of Maximum Wavelength

The maximum absorbance wavelength (λ_{max}) was determined by mixing 5 mL of a 10 mg/L NH_3-N standard solution with 1 mL of Nessler reagent. The mixture was allowed to react, and absorbance was measured using a UV–Vis spectrophotometer over the wavelength range of 300–600 nm.

Calibration Curve Construction

A calibration curve was constructed using NH_3-N standard solutions with concentrations of 0.2, 0.4, 1.0, 1.5, 2.0, and 3.0 mg/L. For each standard, 2 mL of solution was transferred into a test tube, followed by the addition of 1 mL of Nessler reagent, 1.25 mL of sodium potassium tartrate (Rochelle salt), and 0.75 mL of distilled water to obtain a total volume of 5 mL. The mixtures were allowed to react for 10 minutes, and absorbance was measured at 425 nm. Samples with concentrations above

the calibration range were diluted using distilled water before analysis, and the final concentration was calculated by multiplying the measured value by the dilution factor.

Batch Adsorption of Ammonia

Batch adsorption experiments were conducted in 100 mL Erlenmeyer flasks containing 25 mL of NH_3–N solution. A membrane sample (0.1 g) was added, and the mixture was maintained at room temperature (27 °C) under shaking at 200 rpm. For the contact time study, adsorption was conducted for 10, 30, 50, 70, 90, and 110 minutes. For the pH study, adsorption was performed at the equilibrium contact time with pH values adjusted to 3–9 using HCl 0.1 M/NaOH 0.1 M used for pH adjustment. To evaluate the effect of zeolite loading, membranes containing 10%, 20%, and 30% zeolite were used. For the initial concentration study, NH_3–N concentrations were varied at 3, 6, 9, 12, and 15 mg/L. The residual NH_3–N concentration after adsorption was determined using a UV–Vis spectrophotometer (UVmini-1240, Shimadzu) with Nessler reagent. Adsorption performance was expressed in terms of adsorption capacity, following Marlina et al. (2020). All adsorption experiments were conducted in duplicate and the results are presented as mean +/- standard deviation where applicable. The adsorption capacity and removal efficiency were calculated using Equations (2) and (3):

$$q_e = ((C_0 - C_e)V)/m \quad (2)$$

$$\text{Removal efficiency (\%)} = ((C_0 - C_e)/C_0) \times 100 \quad (3)$$

where qe is the adsorption capacity (mg/g), C_0 is the initial NH_3-N concentration (mg/L), C_e is the equilibrium NH_3-N concentration (mg/L), V is the solution volume (L), and m is the mass of membrane adsorbent (g).

Adsorption Isotherms

Langmuir and Freundlich isotherm models were used to evaluate adsorption behavior. The isotherm analysis was performed using equilibrium data obtained from initial NH_3-N concentrations of 3, 6, 9, 12, and 15 mg/L at the optimum contact time. Langmuir parameters were calculated using using the linearized Langmuir equation, while Freundlich parameters were determined using the linearized Freundlich equation. The calculations were based on initial and equilibrium adsorbate concentrations, adsorbent mass, and solution volume. The model parameters were rechecked to ensure consistency between the calculated maximum adsorption capacity and the experimentally observed adsorption capacity. The Langmuir and Freundlich models were expressed as follows:

$$\frac{1}{q_{eq}} = \frac{1}{q_m} + \frac{K_d}{q_m} \times \frac{1}{C_{eq}} \quad (4)$$

$$\log q_e = \log K_F + (1/n) \log C_e \quad (5)$$

where *Ce* is the equilibrium NH_3-N concentration (mg/L), qe is the adsorption capacity at equilibrium (mg/g), q_m is the Langmuir maximum adsorption capacity (mg/g), K_d is the Langmuir affinity constant (L/mg), K_F is the Freundlich adsorption capacity constant, and n is the Freundlich adsorption intensity parameter.

Membrane Regeneration

Membranes exhibiting optimum adsorption performance were subjected to regeneration tests. Desorption of adsorbed species was carried out using NaCl and HCl solutions at concentrations of 1 N, 2 N, and 3 N. The membranes were immersed in the respective solutions and shaken for 1 hour, followed by rinsing with distilled water until neutral pH was achieved and drying in an oven at 70 °C for 3 hours. The regenerated membranes were subsequently evaluated for adsorption performance. Because strong acid may affect cellulose acetate stability, the possible effect of HCl regeneration on membrane integrity was considered in the interpretation of regeneration performance. Regeneration efficiency was calculated using Equation (6):

$$\text{Regeneration efficiency (\%)} = (q_{e,\text{regenerated}}/q_{e,\text{fresh}}) \times 100 \quad (6)$$

where qe, regenerated is the adsorption capacity of the regenerated membrane and qe, fresh is the adsorption capacity of the fresh membrane under the same adsorption conditions. Regeneration was conducted for two consecutive cycles to evaluate reusability.

Adsorption and Filtration Tests Using Palm Oil Mill Effluent

Palm oil mill effluent (POME) samples were collected from the wastewater treatment facility of PT Socfindo Indonesia (Nagan Raya), specifically from the fourth (aerobic) pond. A total of 5 L of wastewater was collected using a plastic container and transferred into a jerry can. Personal protective equipment (PPE) was used during sampling. The samples were stored at [insert actual storage temperature]°C and analyzed within [insert actual holding time] to minimize changes in ammonia-nitrogen concentration. Before UV-Vis analysis, POME samples were diluted using distilled water when necessary to fit within the calibration range. The batch adsorption procedure described above was then applied to the POME samples to evaluate membrane performance under actual wastewater conditions.

For the filtration test, the optimum CA-zeolite MMMA was mounted in a filtration module with an effective membrane area of 0.00255 m2 and operated at 1 bar. The permeate was collected and analyzed for NH3-N concentration using the Nessler method. Removal efficiency for real POME was calculated using Equation (3).

RESULTS AND DISCUSSION

Synthesis of Cellulose Acetate

Cellulose acetate was synthesized from OPEFB-derived cellulose through activation, acetylation, hydrolysis, and precipitation steps. In the activation stage, glacial acetic acid was used as a swelling agent to expand the cellulose fiber structure and increase the accessibility of hydroxyl groups. This treatment facilitates the diffusion of acetic anhydride and sulfuric acid into the cellulose matrix during acetylation (Darmawan et al., 2018). The acetylation reaction was then carried out using acetic anhydride as the acetylating agent and sulfuric acid as the catalyst. During this process, some hydroxyl (–OH) groups in cellulose were substituted by acetyl ($-COCH_3$) groups, resulting in the formation of cellulose acetate (Darmawan et al., 2018).

The acetylation reaction was maintained for 2.5 h to promote acetyl substitution while minimizing possible cellulose degradation or excessive reduction in acetyl content, which may occur under prolonged reaction conditions (Gaol et al., 2013). The subsequent hydrolysis step was performed to remove excess acetyl groups and reduce the formation of sulfuric acid ester by-products. This was achieved by adding glacial acetic acid and distilled water, followed by neutralization of the sulfuric acid catalyst using sodium acetate (Darmawan et al., 2018).

The synthesis produced cellulose acetate as a white powder. From 20 g of cellulose, 40.18 g of cellulose acetate was obtained, corresponding to a product mass yield of 200.9%. The yield exceeding 100% can be attributed to the introduction of acetyl groups into the cellulose structure, which increases the mass of the final derivative relative to the initial cellulose mass. Therefore, this value should be interpreted as product mass yield rather than conversion efficiency. Complete drying and removal of residual reagents are also important to ensure accurate yield determination.

FTIR Analysis of Cellulose Acetate Derived from OPEFB

Fourier Transform Infrared (FTIR) spectroscopy was used to confirm the successful synthesis of cellulose acetate from OPEFB-derived cellulose by identifying changes in characteristic functional groups before and after acetylation. The FTIR spectra of commercial cellulose, OPEFB-derived cellulose, OPEFB-derived cellulose acetate, and commercial cellulose acetate are presented in **Figure 1**.

The spectra of commercial cellulose and OPEFB-derived cellulose show broad absorption bands at 3415 and 3426 cm^{-1}, respectively, corresponding to O–H stretching vibrations associated with hydroxyl groups and hydrogen bonding in cellulose. The bands at 2900 and 2905 cm^{-1} are attributed to aliphatic C–H stretching vibrations. Absorption bands observed at 1366 and 1362 cm^{-1} correspond to C–H bending vibrations, while the bands at 1248 and 1251 cm^{-1} are associated with C–O stretching vibrations in the cellulose structure. The bands at approximately 1640 and 1637 cm^{-1} are attributed to O–H bending vibrations of absorbed water, which are commonly observed in cellulose-based materials.

After acetylation, the OPEFB-derived cellulose acetate spectrum shows a distinct absorption peak at 1745 cm^{-1}, which is assigned to ester carbonyl (C=O) stretching vibrations. This peak is also observed in commercial cellulose acetate at 1759 cm^{-1}, confirming the presence of acetyl groups in the synthesized cellulose acetate. In addition, the absorption band at 1235 cm^{-1} in OPEFB-derived cellulose acetate and 1266 cm^{-1} in commercial cellulose acetate corresponds to C–O stretching of acetyl groups. The band at 1374–1375 cm^{-1} is associated with C–H bending of acetyl methyl groups, while the bands at 2954 and 2949 cm^{-1} correspond to aliphatic C–H stretching.

The similarity between the FTIR spectrum of OPEFB-derived cellulose acetate and that of commercial cellulose acetate indicates that cellulose extracted from OPEFB was successfully converted into cellulose acetate. The appearance of the ester carbonyl peak at 1745 cm^{-1}, together with the C–O acetyl absorption band at 1235 cm^{-1}, provides strong evidence of successful acetylation.

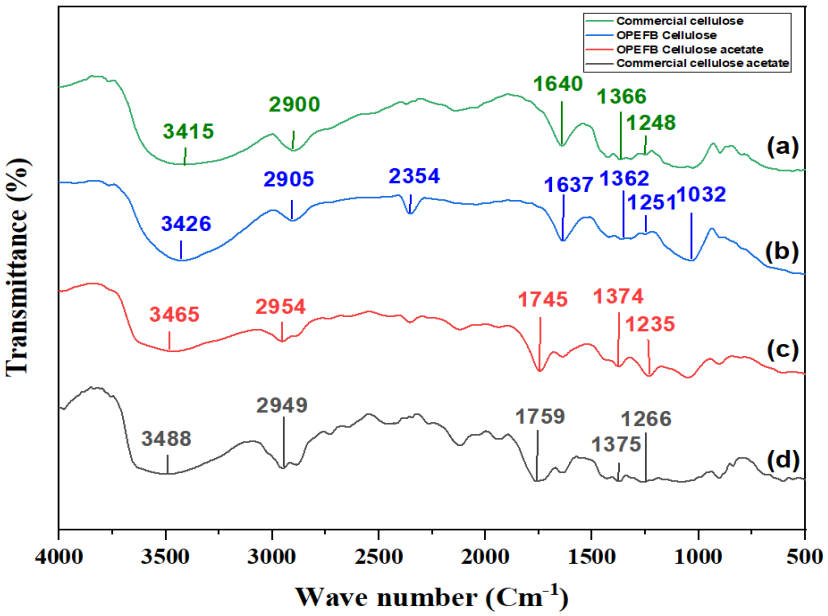

Figure 1. FTIR spectra of **(a)** commercial cellulose, **(b)** OPEFB-derived cellulose, **(c)** OPEFB-derived cellulose acetate, and **(d)** commercial cellulose acetate. The appearance of ester carbonyl peaks at approximately 1745–1759 cm^{-1} and C–O acetyl peaks at approximately 1235–1266 cm^{-1} confirms the successful acetylation of cellulose.

Figures 1(a) and **1(b)** present the FTIR spectra of commercial cellulose and OPEFB-derived cellulose, respectively. The absorption band at approximately 3415–3426 cm^{-1} corresponds to O–H stretching vibrations, indicating the presence of hydroxyl groups and hydrogen bonding within the cellulose structure (Haafiz et al., 2013; Filho et al., 2008; Lismeri et al., 2016). The absorption bands at 2900–2905 cm^{-1} are attributed to C–H stretching vibrations of CH_2 groups of an aliphatic chain. Additionally, bands at 1362–1366 cm^{-1} correspond to CH_2 bending vibrations, reflecting structural deformation in cellulose (Aditama et al., 2017), while bands at 1248–1251 cm^{-1} are associated with C–H bending vibrations (Haafiz et al., 2013).

Figures 1(c) and **1(d)** show the FTIR spectra of cellulose acetate derived from OPEFB and commercial cellulose acetate, respectively. The appearance of a strong absorption peak at approximately 1745 cm^{-1} in OPEFB-derived cellulose acetate, and at 1759 cm^{-1} in commercial cellulose acetate, indicates the presence of carbonyl (C=O) groups, which are characteristic of ester

carbonyl functionalities in cellulose acetate (Lismeri et al., 2016). Furthermore, absorption bands at 1235 cm^{-1} (OPEFB-derived) and 1266 cm^{-1} (commercial) confirm the presence of C–O stretching vibrations associated with acetyl groups (Ginting et al., 2023). The band observed at approximately 3465 cm^{-1} corresponds to residual O–H groups, indicating incomplete substitution of hydroxyl groups, while the peak at 2954 cm^{-1} is attributed to aliphatic C–H stretching vibrations. The similarity between the FTIR spectra of OPEFB-derived cellulose acetate and commercial cellulose acetate confirms the successful acetylation of cellulose. A detailed comparison of functional groups is presented in **Table 2**.

Table 2. FTIR functional group analysis of OPEFB-derived and commercial cellulose acetate

Wavenumber (Cm^{-1})				Vibrational assignment	Description
Commercial Cellulose	OPEFB Cellulose	OPEFB Cellulose Acetate	Commercial Cellulose Acetate		
3415	3426	3465	3488	O-H stretching	Alcohols, phenols
2900	2905	2954	2949	C-H stretching	Aliphatic C-H stretching
1640	1637	1745	1759	C=O stretching	Ester carbonyl of cellulose acetate
1366	1362	1374	1375	C-H bending	$-CH_2$ from cellulose
1248	1251	1235	1266	C-O acetyl	Alcohols, ester, carboxylic acids, anhydrides

Characterization of Natural Zeolite

XRD Analysis

X-ray diffraction (XRD) analysis was conducted to determine the crystalline structure of the natural zeolite before and after activation. The diffraction patterns are presented in **Figure 2**, while the corresponding 2θ data are summarized in **Table 3**.

Table 3. 2θ data of natural zeolite before and after activation

Before Activation		After Activation	
2θ	Desc	2θ	Desc
13,38	Zeo-M	13,42	Zeo-M
19,61	Zeo-M	19,56	Zeo-M
20,79	O_2Si-Q	20,73	O_2Si-Q low
22,17	Zeo-M	22,19	Zeo-M
-	-	23,7	O_2Si-Q
25,54	Zeo-M	25,50	Zeo-M
26,57	O_2Si-Q	26,56	O_2Si-Q low
27,53	Zeo-M	27,61	Zeo-M
30,83	Zeo-M	30,79	Zeo-M
35,56	Zeo-M	35,66	Zeo-M
36,50	O_2Si-Q	36,34	O_2Si-Q low
-	-	39,37	O_2Si-Q

These results correspond to JCPDS database references 96-153-1897(Ca_3.4 (Al_7.4 Si40.6 O96) (H_2O)31), 96-900-0777 (SiO_2), and low-quartz SiO_2 standards. The activated zeolite exhibited well-defined diffraction peaks, indicating increased crystallinity, which is consistent with Renni et al. (2018). The activation process may remove impurities and improve pore accessibility, thereby improving the zeolite's adsorption performance (Renni et al., 2018). Another characteristic feature of zeolites is the presence of diffraction peaks at 2θ values between 0° and 50°, with sharp peaks typically observed at angles between 20° and 30° (Ojumu et al., 2016). In this study, both samples exhibited peaks within this range; however, the difference in peak intensity between the activated and unactivated zeolite at 2theta approximately 25.6° was small; therefore, successful activation was interpreted together with SEM-EDS evidence rather than from peak intensity alone.

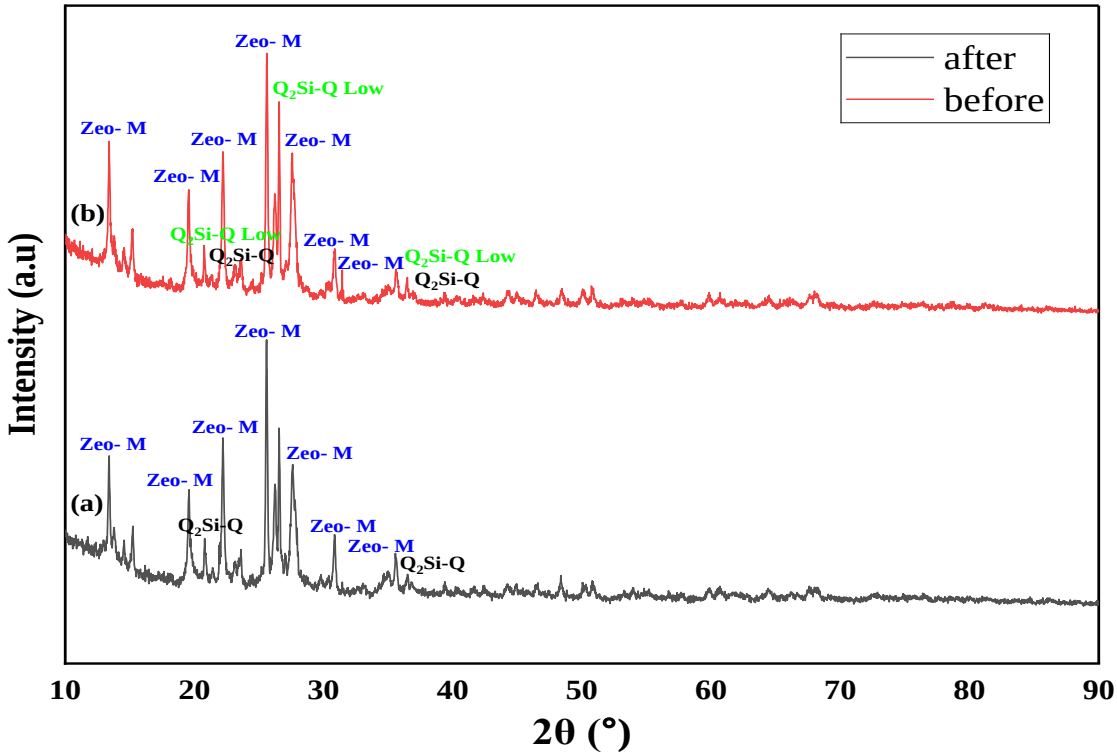

Figure 1. XRD diffractograms of natural zeolite before and after activation

Mordenite is a microporous zeolite with an orthorhombic crystal structure and well-defined channels that facilitate the transport of water molecules and relatively large ions (Muttaqi et al., 2019). Due to its channel structure, mordenite functions effectively as both a molecular sieve and an adsorbent (Atikah, 2017). Its exchangeable cations also make it suitable for ammonium removal through ion-exchange mechanisms.

SEM-EDS Analysis

Scanning Electron Microscopy–Energy Dispersive X-ray (SEM–EDS) analysis was performed to evaluate the morphology and elemental composition of natural zeolite before and after activation.

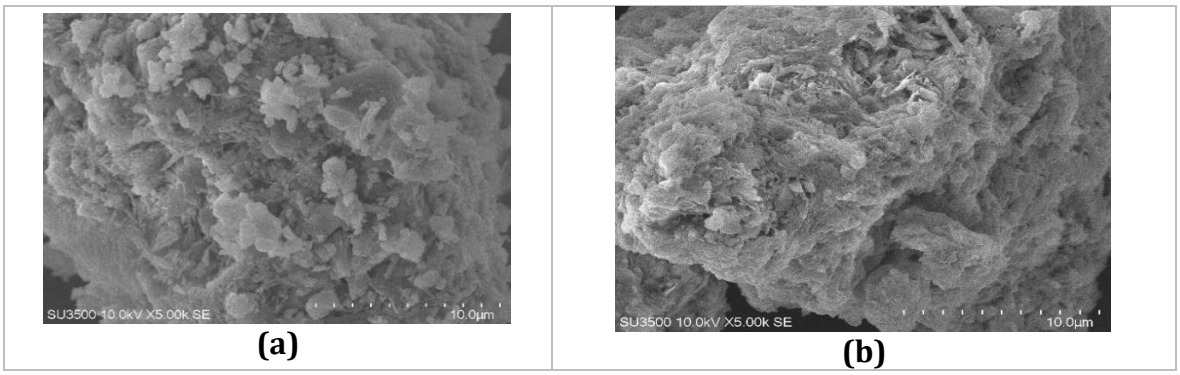

Figure 2. Morphology of Klaten natural zeolite: (a) before activation and (b) after activation

As shown in **Figure 3(a)**, the unactivated zeolite surface was covered with impurities that blocked pore openings. In contrast, **Figure 3(b)** shows that the activated zeolite exhibited a cleaner and more ordered surface with more clearly defined pores. This observation is consistent with Setiawan et al. (2018), who reported that calcination effectively removes surface impurities. These impurities, which may include organic and inorganic compounds, are typically eliminated during acid activation (Septommy and Badriyah, 2022), thereby improving pore accessibility and adsorption performance (Sofith et al., 2020). Although BET surface area was not measured in this study, the SEM observation suggests improved surface accessibility after activation.

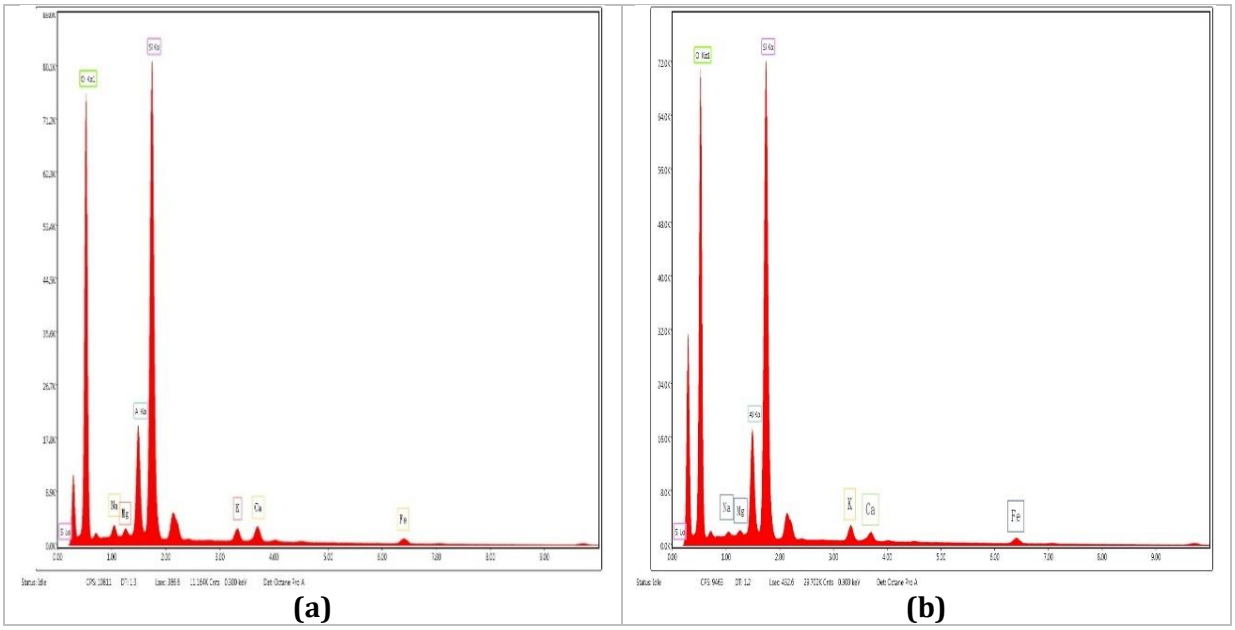

Figure 3. SEM–EDS analysis of zeolite: (a) before activation and (b) after activation

The SEM–EDS results **(Figures 4a** and **4b)** indicate changes in elemental composition following activation. The concentrations of Mg and Ca decreased after activation decreased after activation, likely due to ion exchange between zeolite cations and H^+ ions from HCl (Septommy and Badriyah, 2022). Al decreased slightly, while K and Fe increased in relative percentage, which may reflect the removal of other components and the semi-quantitative nature of EDS analysis rather than absolute enrichment. Acid treatment facilitates the dissolution of oxide impurities and enhances pore structure, resulting in improved pore accessibility and improved adsorption capacity. Based on **Table 4**, Si and O were the dominant elements in both samples. After activation, the zeolite composition was dominated by O (43.15%), Si (39.56%), and Al (87.86%), which is consistent with the typical aluminosilicate framework of zeolites. A higher Si content is associated with improved stability and increased surface polarity, which enhances adsorption performance (Septommy and Badriyah, 2022). Other elements, such as K, Fe, and Ca, represent exchangeable cations associated with the zeolite framework.

Table 4. Elemental composition of natural zeolite before and after activation based on SEM-EDS analysis

Type of zeolite	Mineral Composition (%)						
	O	Mg	Al	Si	K	Ca	Fe
Before activation	42.12	0.14	8.12	39.53	2.45	3.90	3.76
Activated zeolite	43.15	0.01	7.86	39.56	3.01	2.24	4.17

Preparation of Pure and Adsorptive Membranes

Membrane fabrication was carried out using the phase inversion method, in which a polymer solution is transformed into a solid membrane through controlled phase separation (Bahmid et al., 2013). The physical appearance of pure cellulose acetate membranes (CA 0%) and zeolite-modified membranes (CA–Z10%, CA–Z20%, and CA–Z30%) is shown in **Figure 5**. The pure cellulose acetate membrane exhibited a uniform white appearance, whereas the cellulose acetate–zeolite membranes showed a slightly yellowish color. Morphologically, the modified membranes exhibited a denser surface with a slightly fibrous texture. This difference is attributed to the incorporation and distribution of activated zeolite particles within the membrane matrix and on the membrane surface. At higher zeolite loading, particle agglomeration may occur and may influence membrane morphology, permeability, and mechanical properties.

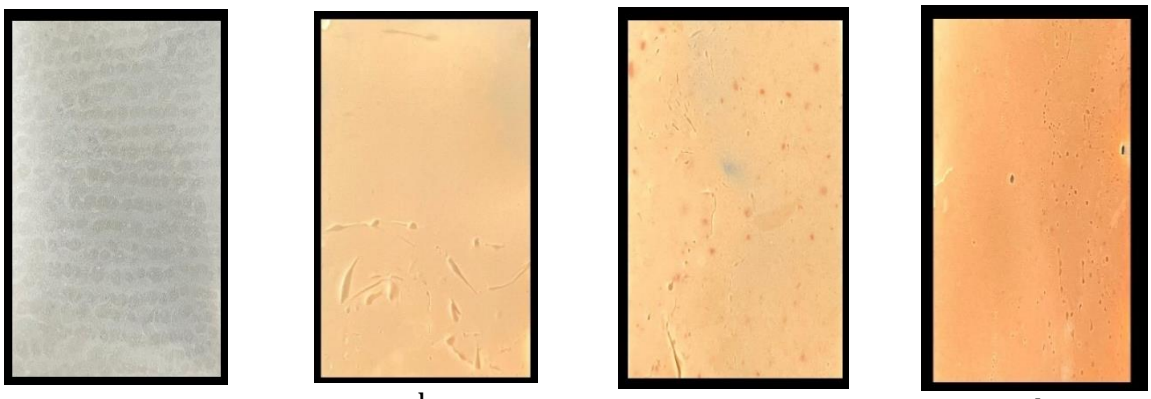

Figure 4. Membrane **(a)** CA 0% (b) CA-Z 10% (c) CA-Z 20% (d) CA-Z 30%

Membrane Characterization

Membrane Permeability (Flux Test)

Membrane permeability was evaluated through pure water flux measurements using pristine cellulose acetate (CA) membranes and cellulose acetate–zeolite mixed matrix membranes (MMMAs). The membranes had an effective surface area of 0.00255 m^2 and were tested under an applied pressure of 1 bar. The results are presented in **Figure 6**. Flux data are shown for the pristine CA membrane and the CA-zeolite MMMA with 30% zeolite loading, which was selected based on its best adsorption performance.

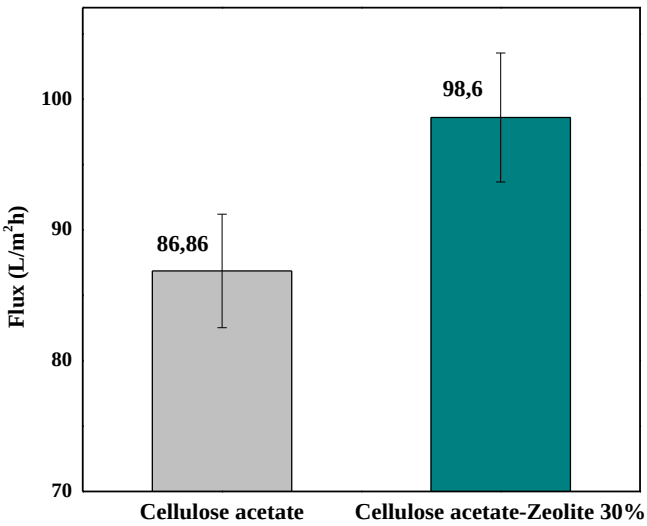

Figure 5. Flux performance of pristine CA and CA–zeolite MMMAs with 30% zeolite loading

The pristine CA membrane exhibited a lower flux (86.86 $L \cdot m^{-2} \cdot h^{-1}$) compared to the CA–zeolite MMMA (98.60 $L \cdot m^{-2} \cdot h^{-1}$). The increased flux in the mixed matrix membrane is attributed to the incorporation of zeolite, which enhances membrane porosity and permeability. The presence of zeolite particles contributes to the formation of additional transport pathways and enlarged pore structures, thereby facilitating higher water flux. However, flux values for all zeolite loadings should be reported in future work to provide a more complete understanding of the relationship between filler loading and permeability.

Swelling Degree and Porosity

The swelling degree and porosity of pristine CA membranes and CA–zeolite MMMAs (30% loading) are presented in **Figure 7**.

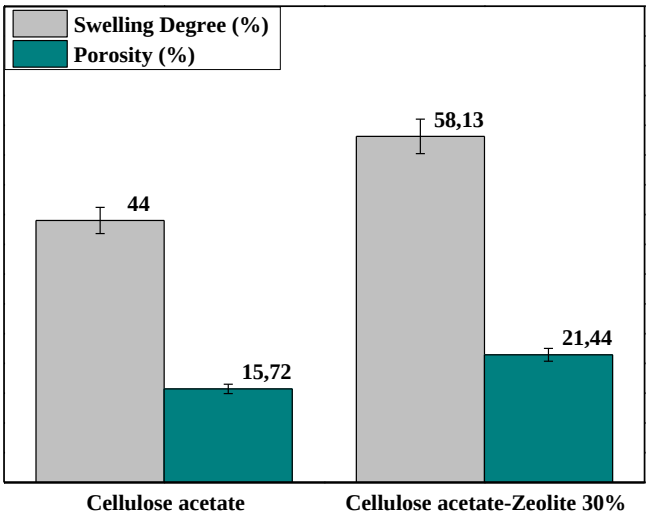

Figure 6. Swelling degree and membrane porosity of pristine CA and CA-zeolite MMMAs with 30% zeolite loading

The swelling degree of pristine CA membranes and CA–zeolite MMMAs (30%) was 44% and 58.13%, respectively. These values are higher than those reported in previous studies, such as (26.15% and 33.47%) and (38.89% and 41.44%) (Saiful et al., 2024). The porosity values for pristine and modified membranes were 15.72% and 21.44%, respectively. The increase in porosity in CA–zeolite MMMAs is attributed to interactions between zeolite particles and the polymer matrix, which create additional voids and increase inter-chain spacing. This results in a more open membrane structure. The increased porosity also enhances membrane hydrophilicity, leading to a higher swelling degree (Ho et al., 2025). These results indicate that zeolite incorporation improved water uptake and permeability-related properties, although these improvements must be evaluated together with the mechanical-property changes discussed below.

Membrane Tensile Strength

Tensile testing was conducted to evaluate the mechanical properties of the membranes, including tensile strength and elongation. The test was performed on pure cellulose acetate membranes and cellulose acetate–zeolite MMMAs (30%), which exhibited the best adsorption performance. The results are shown in **Figure 8**.

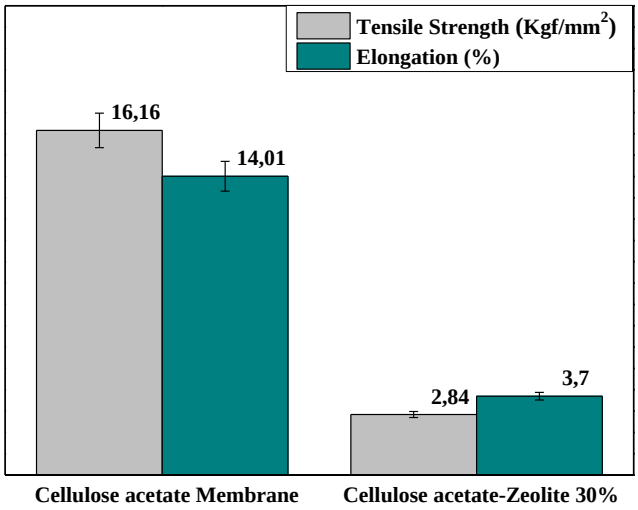

Figure 7. Tensile properties of pristine CA membranes and CA–zeolite MMMAs with 30% zeolite loading

The pristine CA membrane exhibited higher tensile strength (16.16 kgf·mm^{-2}) compared to the CA–zeolite MMMA (2.84 kgf·mm^{-2}). This reduction in mechanical strength may be attributed to

non-uniform membrane thickness and the presence of zeolite particles that are not fully integrated into the polymer matrix, which can induce brittleness. Similarly, elongation at break decreased from 14.01% for the pristine membrane to 3.70% for the modified membrane, indicating reduced flexibility upon zeolite incorporation. Therefore, zeolite incorporation did not improve all membrane properties. Instead, it produced a trade-off: adsorption-related properties, swelling degree, porosity, and flux increased, whereas tensile strength and elongation decreased. This mechanical weakening may be associated with weak interfacial compatibility between cellulose acetate and zeolite, particle agglomeration, and defect formation within the polymer matrix.

Morphological Analysis (SEM)

Scanning Electron Microscopy (SEM) was used to examine membrane morphology, including surface and cross-sectional structures, for both pristine CA membranes and CA–zeolite MMMAs (30%). The results are presented in **Figure 9**. The pristine CA membrane exhibited a relatively smooth surface with limited visible pores, while the CA–zeolite MMMA showed a rougher surface due to the dispersion of zeolite particles. The bottom surface of the membranes appeared smoother and less porous than the top surface. The rougher top surface indicates the presence of zeolite particles on or near the membrane surface, which may increase the number of available adsorption sites for ammonium species.

The cross-sectional structure of the CA–zeolite membrane was denser, which may be attributed to increased solution viscosity and zeolite agglomeration during membrane casting. These factors slow solvent–non-solvent exchange during phase inversion, resulting in a denser structure (Amira et al., 2021). In addition, the surface of the cellulose acetate–zeolite MMMAs appeared rougher than that of the pristine cellulose acetate membrane due to the dispersion of zeolite particles across the membrane surface and within the pore layers. The increased surface roughness and presence of zeolite particles are expected to enhance ammonia adsorption capacity. The denser cross-section does not necessarily contradict the increased porosity and flux, because additional interfacial voids and surface pores around zeolite particles may improve water transport even when parts of the cross-section appear compact.

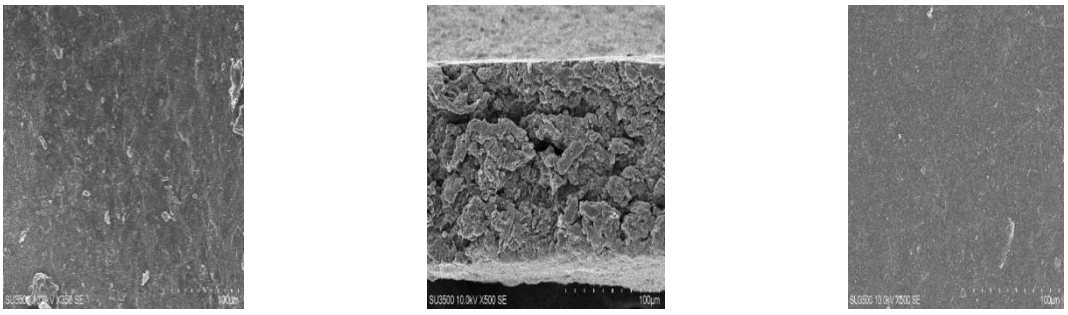

Top surface Cross-section Bottom surface

(a)

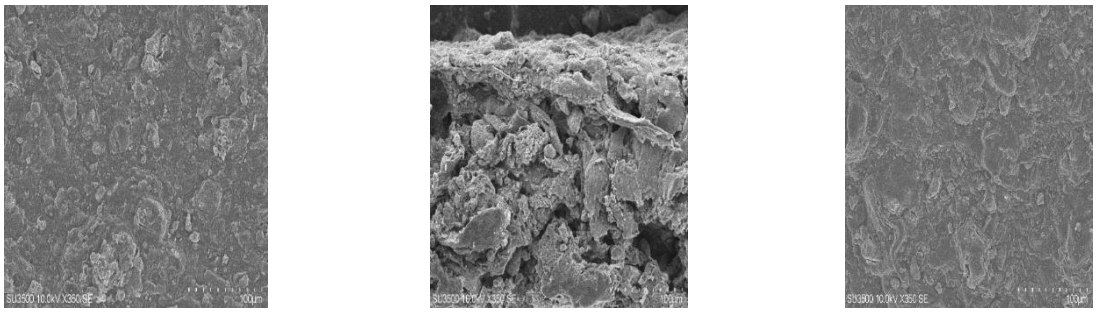

Top surface Cross-section Bottom surface

(b)

Figure 8. SEM images of **(a)** pristine CA membrane and **(b)** CA–zeolite MMMAs with 30% zeolite loading

FTIR Analysis

Fourier Transform Infrared (FTIR) analysis was performed to identify functional groups and confirm the incorporation of zeolite into the cellulose acetate membrane matrix. The spectra are presented in **Figure 10**. **Figure 10 (a)** and **(b)** show the spectra of cellulose acetate membranes and zeolite-modified cellulose acetate membranes, respectively. The cellulose acetate membrane was successfully identified by the absorption band at 3439.23 cm^{-1}, corresponding to hydroxyl (O–H) groups. This is consistent with previous studies by Safiah., & Sri, M. (2018), who reported O–H groups at 3380 cm^{-1}, and Amira et al. (2021) at 3484 cm^{-1}. The absorption at 1741.80 cm^{-1} indicates the presence of ester carbonyl (C=O) groups in cellulose acetate, in agreement with Safiah., & Sri, M. (2018) at 1750 cm^{-1} and Batu et al. (2023) in the range of 1738-1751 cm^{-1}. Furthermore, the band at 1374.34 cm^{-1} corresponds to C-H bending vibrations of the cellulose acetate structure, consistent with Amira et al. (2021), who reported bending vibrations at 1434 cm^{-1}, and Safiah., & Sri, M. (2018) at 1380 cm^{-1}. Ester functional groups (C–O) appear at 1233.53 cm^{-1} and 1035.82 cm^{-1}, in agreement with Amira et al. (2021), who identified ester groups at 1054 cm^{-1} originating from glycosidic units, and Safiah., & Sri, M. (2018), who reported peaks at 1050 and 1240 cm^{-1}.

Figure 10(b) shows that the spectrum of zeolite-modified cellulose acetate membranes exhibits shifts in wavenumbers for each functional group due to the addition of zeolite. The hydroxyl group appears at 3425.72 cm^{-1}, carbonyl (C=O) at 1743.72 cm^{-1}, C-H vibration at 1376.27 cm^{-1}, and ester (C–O) at 1226.78 cm^{-1} and 1057.04 cm^{-1}. Additionally, a new functional group, Si–O, appears at 803.16 cm^{-1}, indicating the presence of zeolite within the cellulose acetate membrane and confirming the success of the modification process. This finding is supported by Amira et al. (2021), who reported Si–O groups at 906 cm^{-1}. A detailed comparison of functional groups is presented in **Table 5**.

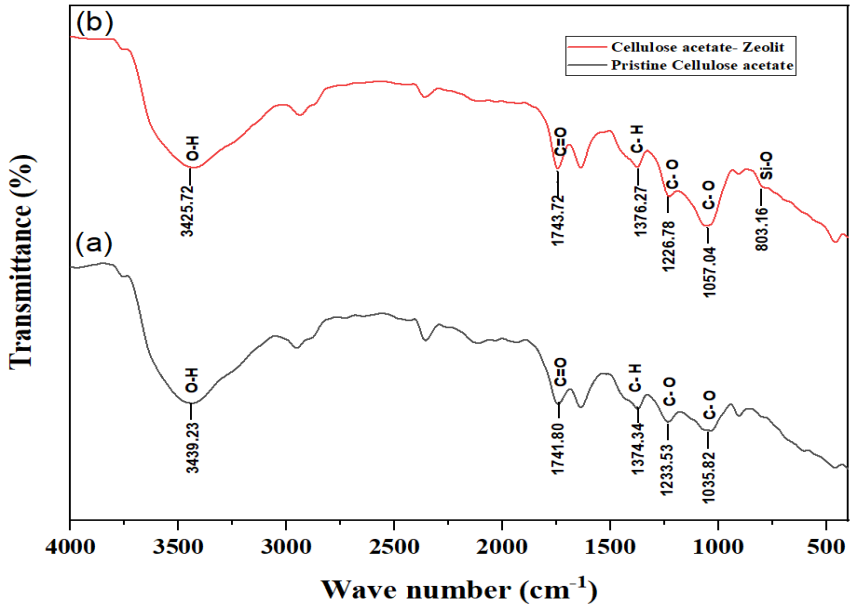

Figure 9. FTIR spectra of (a) Pristine CA membrane and (b) CA–zeolite membrane

Table 5. FTIR functional group analysis of pristine CA and CA–zeolite

Wavenumber (cm^{-1})		Functional Group	Description
Pure cellulose acetate	Cellulose acetate–zeolite		
3439	3425	O-H stretching	Alcohol, phenol
1741	1743	C=O stretching	Ester carbonyl of cellulose acetate
1374	1376	C-H stretching	-CH_2 from cellulose
1233	1226	C-O acetyl	Alcohol, ester, carboxylic acid, anhydride
1035	1057	C-O acetyl	Alcohol, ester, carboxylic acid, anhydride
-	803	Si-O	Silanol (zeolite)

Adsorption Performance

Effect of Contact Time

The optimum contact time was determined by evaluating adsorption capacity at different contact times between the membrane and a 6 mg/L NH_3-N solution. The contact time variations used in this study were based on Nurman et al. (2021) for 10, 30, 50, 70, 90, and 110 minutes. The results are presented in **Figure 11**.

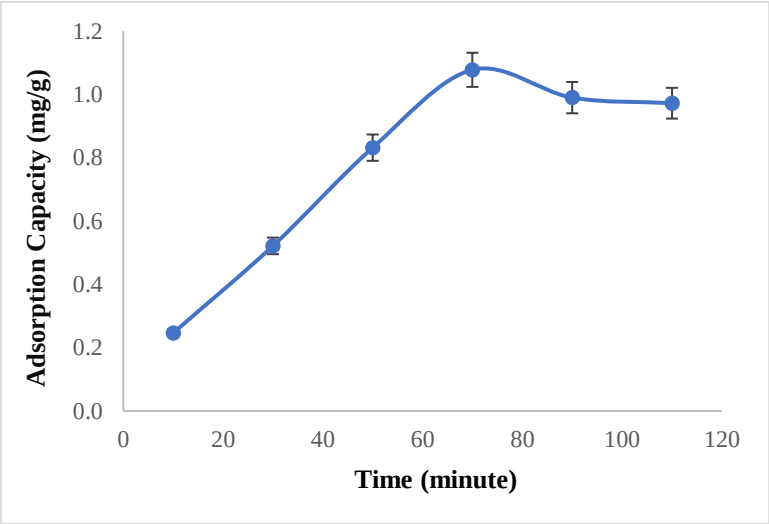

Figure 10. Effect of contact time on NH_3-N adsorption capacity

As shown in **Figure 11**, the adsorption capacity increased with contact time. The highest adsorption capacity was achieved at 70 minutes, reaching 1.0779 mg/g, which was identified as the optimum contact time. Beyond this point, the adsorption capacity decreased slightly at 90 minutes to 0.990 mg/g and remained relatively constant at 110 minutes. This behavior indicates that equilibrium was reached at approximately 70 minutes, after which the active sites on the membrane became saturated. The subsequent decrease in adsorption capacity may be attributed to weak interactions between ammonium species and the adsorbent surface, leading to partial desorption (Nuryoto et al., 2020). This value represents the adsorption capacity obtained in the contact-time experiment using 6 mg/L NH_3-N and should be distinguished from capacities obtained under different initial concentrations or material comparisons.

Effect of Zeolite Loading Percentage

The zeolite loading percentage, defined as the proportion of zeolite incorporated into the membrane matrix, significantly influences adsorption capacity. The effect of zeolite loading on NH_3-N adsorption is presented in **Figure 12**.

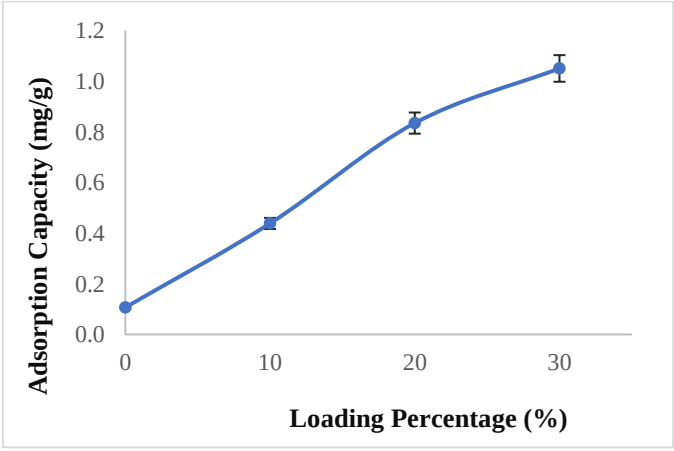

Figure 11. Effect of zeolite loading percentage on NH_3-N adsorption capacity

As shown in **Figure 12**, adsorption capacity increased with increasing zeolite loading. The cellulose acetate–zeolite MMMA with 10% loading exhibited an adsorption capacity of 0.439 mg/g, while the 30% loading reached 1.051 mg/g. This trend is attributed to the higher number of available active sites provided by increased zeolite content, thereby enhancing the adsorption of ammonium species through adsorption and ion-exchange interactions (Maelan et al., 2024). Although 30% zeolite loading produced the highest adsorption capacity among the tested membranes, excessive filler loading may increase particle agglomeration and weaken mechanical properties, as indicated by the tensile test results.

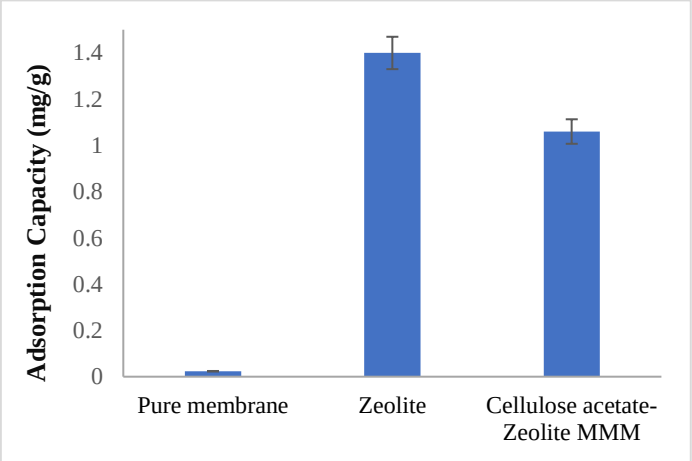

Figure 12. NH_3-N Adsorption capacity of pristine membrane, zeolite, and CA–zeolite MMMAs

Based on **Figure 13**, the pure cellulose acetate membrane exhibited a low adsorption capacity, while zeolite-containing materials showed higher adsorption capacity. The adsorption capacity values should be interpreted according to the tested material and experimental condition to avoid confusion among the values obtained from contact-time, loading, concentration, and material-comparison experiments. This result indicates that zeolite has strong potential as an adsorbent for reducing ammonia levels in palm oil mill effluent (POME). **Table 6** presents a comparison of natural zeolites used in different studies for ammonia or ammonium adsorption.

Table 6. Comparison of ammonia adsorption capacities of various natural zeolites

Type of Zeolite	Mineral Phase	Adsorbate	Adsorption Capacity (Mg/G)	Reference
Natural zeolite	Clinoptilolite	NH_3	13,4	Wang & Peng, (2010)
Natural zeolite	Clinoptilolite	NH_3	10,8	Zhou & Boyd, (2014)
Natural zeolite	Mordenite	NH_3	0,42	Amini et al., (2017)
Natural zeolite	Mordenite	NH_3	1,40	This study

The pure cellulose acetate membrane exhibits a very low adsorption capacity of 0.024 mg/g, highlighting the need for the incorporation of activated natural zeolite to enhance performance. The combination of cellulose acetate membranes with zeolite powder yields a high adsorption capacity of 1.051 mg/g under the selected zeolite-loading condition, whereas powdered zeolite showed an adsorption capacity of 1.40 mg/g under the material-comparison test. These values confirm that zeolite is the main contributor to NH_3-N adsorption, while the cellulose acetate matrix provides the membrane structure for filtration and handling.

Effect of pH

The degree of acidity (pH) is a critical parameter in adsorption processes, influencing the distribution of ammonia species, especially the equilibrium between $NH4^+$ and NH_3, as well as the activity of functional groups on the membrane. Adsorption capacity generally decreases with increasing acidity (Cozmuta et al., 2012). The effect of pH is shown in **Figure 14**.

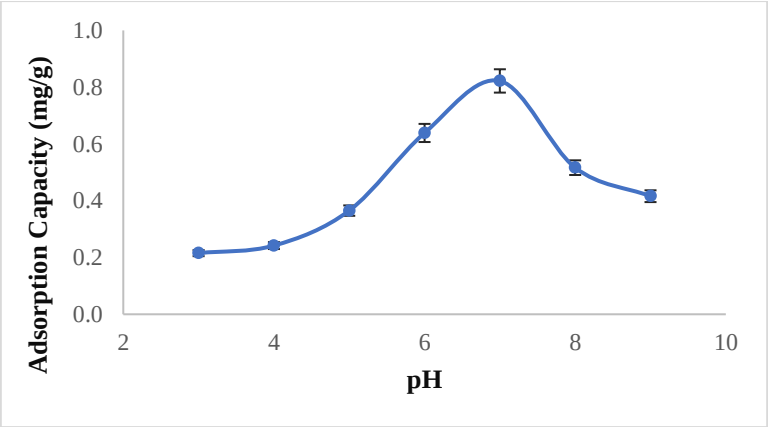

Figure 13. Effect of pH on NH_3-N adsorption capacity

As illustrated in **Figure 14**, the highest adsorption capacity was achieved at pH 7, with a qe value of 0.822 mg/g. This finding is consistent with Marlina et al. (2020). At lower pH values (pH 6), adsorption capacity decreased, and a significant decline was observed at pH 8. At acidic to neutral pH, ammonia nitrogen predominantly exists as NH_4^+, whereas the proportion of unionized NH_3 increases under alkaline conditions. Because natural zeolite commonly removes ammonium through cation exchange, adsorption at pH 7 may be favored by the availability of $NH4^+$ and sufficient active exchange sites on the zeolite surface. Under more acidic conditions, excess H^+ may compete with NH_4^+ for exchange sites, reducing adsorption capacity. Under more alkaline conditions, the increasing fraction of NH_3 and possible changes in surface interaction may also reduce removal efficiency. The pHpzc concept should be interpreted cautiously because the pHpzc value of the membrane was not measured in this study. Therefore, pH 7 was selected as the optimum condition for subsequent experiments.

Effect of Initial Concentration

The optimum adsorbate concentration was determined by varying NH_3-N concentrations (3, 6, 9, 12, and 15 ppm), using 0.1 g of adsorbent and a contact time of 70 minutes. The results are shown in **Figure 15**.

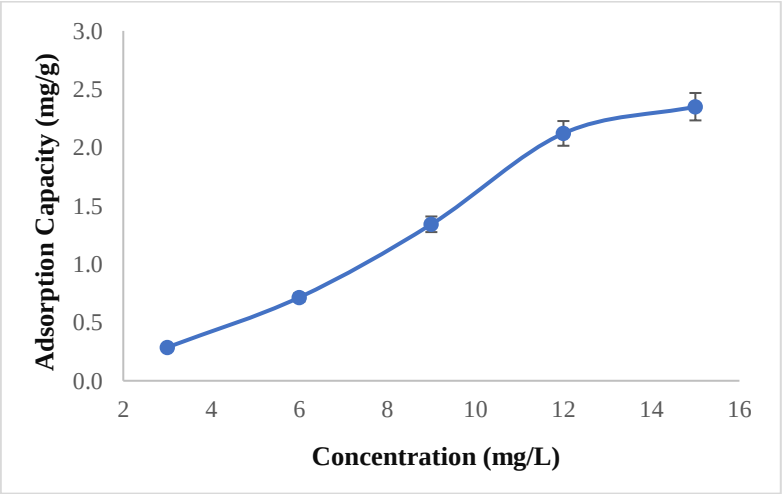

Figure 14. Effect of initial NH_3-N concentration on adsorption capacity

Figure 15 shows that adsorption capacity increases with increasing initial NH_3-N concentration, from 0.287 mg/g at 3 mg/L to 2.350 mg/g at 15 mg/L. This trend indicates a direct relationship between initial concentration and adsorption capacity. Higher concentrations increase the concentration gradient and provide more $NH4^+$ ions available for adsorption and ion exchange with active sites on the zeolite-containing membrane, leading to increased adsorption (Raja, 2016).

Thus, the optimum adsorption capacity was achieved at an initial concentration of 15 mg/L. This value was obtained from the initial-concentration experiment and should not be directly compared with the 1.051 mg/g value obtained under the selected zeolite-loading condition without considering differences in experimental conditions.

Adsorption Kinetics

The kinetics of NH_3-N adsorption were analyzed using two common models: pseudo-first-order (PFO) and pseudo-second-order (PSO). The results are presented in **Figure 16** and **Table 7**.

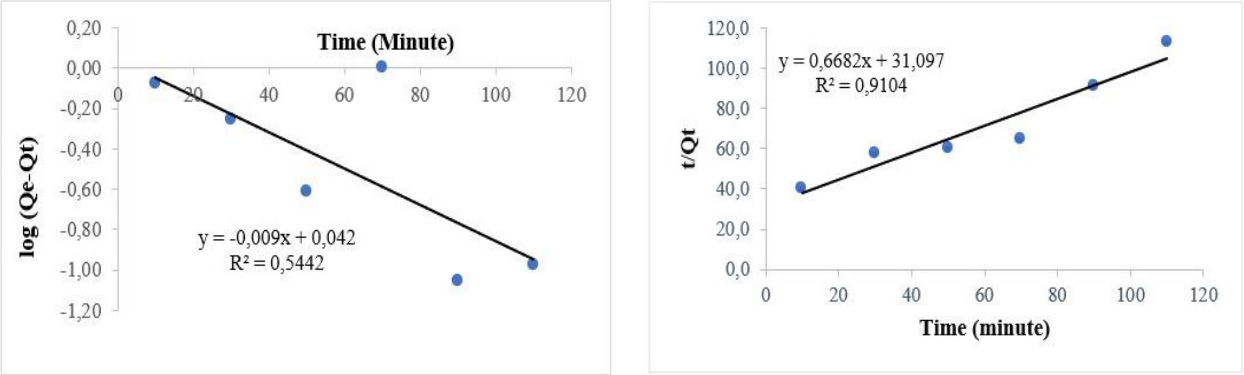

a b

Figure 15. Adsorption kinetics models: pseudo-first-order (PFO) **(a)** and pseudo-second-order (PSO) **(b)**

Based on **Table 7**, the qe value for the pseudo first order (PFO) model is 1.015 mg/g, with a rate constant (k) of 0.0207 min^{-1}, indicating that 1 g of adsorbent can adsorb 0.0207 mg of adsorbate per minute. For the pseudo second order (PSO) model, the qe value is 1.4965 mg/g, with a rate constant of 0.0215 g mg^{-1} min^{-1}. The coefficient of determination (R^2) for PFO is 0.5442, while the PSO model shows a higher R^2 of 0.9104, indicating a better empirical fit than the PFO model. Therefore, NH_3-N adsorption using cellulose acetate–zeolite MMMAs is better described by the pseudo-second-order model. However, PSO fitting alone does not conclusively prove chemisorption; it indicates that the adsorption rate may be associated with the availability of surface active sites and interactions between NH4+ and the zeolite-containing membrane (Rosa et al., 2012).

Table 7. Adsorption kinetics parameters

Parameter	Pseudo-first-order (PFO)	Pseudo-second-order (PSO)
qe	1,015 mg/g	1,4965 mg/g
K	0.0207 min^{-1}	0,0215 g mg^{-1} min^{-1}
R^2	0,5442	0,9104

Adsorption Isotherms

Adsorption behavior was evaluated using the Langmuir and Freundlich isotherm models. The Langmuir isotherm was determined by plotting 1/Ce versus 1/Qe, while the Freundlich isotherm for NH_3-N adsorption using the CA-zeolite MMMAs with 30% zeolite loading was obtained by plotting log qe versus log Ce based on batch adsorption data at varying initial NH_3-N concentrations. The corresponding plots are presented in **Figure 17**, and the calculated parameters are summarized in Table 8. The isotherm parameters should be verified to ensure consistency between the fitted Langmuir maximum capacity and the experimentally observed adsorption capacity.

Table 8. Adsorption isotherm parameters

Freundlich Isoterm			Langmuir Isoterm		
K_F	n	R^2	Qm (m/g)	b	R^2
0,0944	0,4978	0,8351	0,6131	0,1773	0,9247

Note: K_F (Freundlich constant), n (adsorption intensity), Qm (maximum adsorption capacity), b (Langmuir constant) and R^2 (regression coefficient).

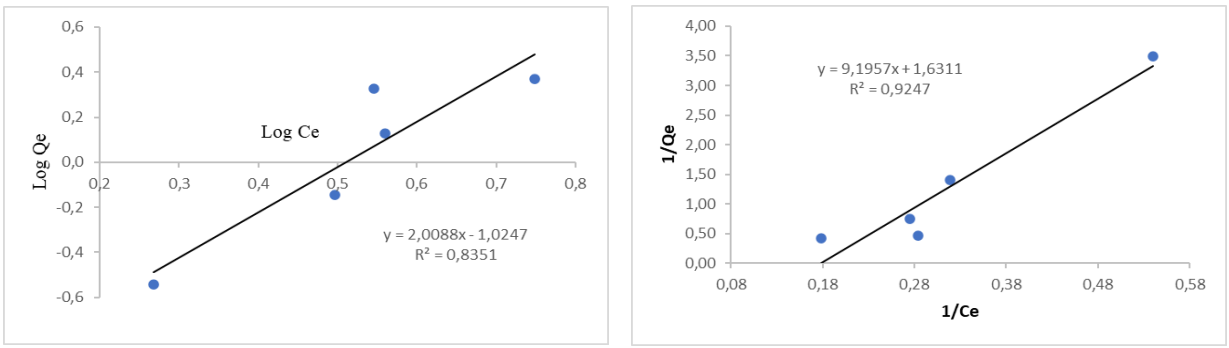

a b

Figure 17. Freundlich (a) and Langmuir (b) adsorption isotherm models

Based on **Table 8**, the coefficient of determination (R^2) indicates that NH_3-N adsorption using cellulose acetate–zeolite MMMAs is better described by the Langmuir isotherm model, as evidenced by an R^2 value of 0.9247 (close to 1). According to the Langmuir isotherm parameters, the maximum adsorption capacity (Qm) was determined to be 0.6131 mg/g, representing the maximum amount of adsorbate that can be adsorbed onto a monolayer surface. However, this Qm value is lower than the experimentally observed adsorption capacity at 15 mg/L; therefore, the Langmuir calculation, units, and linear fitting should be rechecked before drawing a strong conclusion regarding maximum capacity. The Langmuir constant (b) value of 0.1773 indicates interaction between the adsorbate and adsorbent surface. However, the moderate value of b suggests that the interaction is not particularly strong, implying that the adsorption process is likely dominated by physical interactions and ion-exchange contributions, rather than strong chemical bonding. Furthermore, the Freundlich constant (*Kf*) value of 0.0944 and the n value of 0.4978 ($n < 1$) require cautious interpretation because favorable adsorption is commonly associated with $n > 1$ or $0 < 1/n < 1$, depending on the equation form used. Therefore, the Freundlich parameter interpretation should be verified. Nevertheless, since the R^2 value of the Langmuir model is higher, the adsorption process is better described by the Langmuir isotherm, indicating possible monolayer adsorption on a relatively homogeneous surface (Aulia et al., 2021).

Membrane Regeneration

In this study, NaCl and HCl solutions with concentrations of 1 N, 2 N, and 3 N were used as regenerating agents, with an immersion time of 60 minutes. The regeneration process was conducted for two consecutive cycles, in which the membrane regenerated in the first cycle was reused for the second regeneration cycle and subsequently tested using a standard NH_3-N solution with a concentration of 6 ppm.

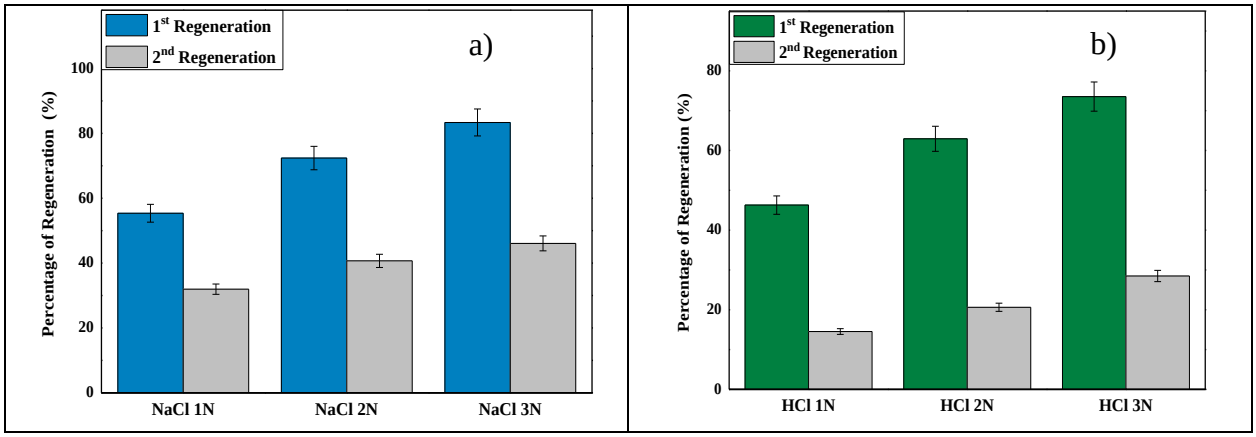

Figure 18. Regeneration performance of cellulose acetate–zeolite MMMAs using (a) NaCl and (b) HCl

The adsorption capacity under optimal conditions, obtained from previous experiments, was used as a reference to evaluate regeneration efficiency. The results indicate a clear difference in

performance between the two regenerating agents. Regeneration with NaCl consistently resulted in higher regeneration efficiency compared to HCl. The highest regeneration efficiency was achieved using 3 N NaCl, reaching 83.37%, whereas the optimum performance for HCl was also observed at 3 N, with a lower efficiency of 73.52%. These results indicate that the regenerated cellulose acetate–zeolite MMMAs can still be used effectively as an NH_3-N adsorbent; however, its adsorption capacity decreased slightly compared to that of the fresh membrane. Furthermore, the membrane subjected to the second regeneration cycle exhibited a further decline in adsorption performance compared to the first regeneration cycle. In the second regeneration, the maximum regeneration efficiency was obtained with 3N NaCl (46.08%), while regeneration with 3N HCl resulted in 28.47%.

The results indicate that membrane regeneration in the first cycle maintains good adsorption performance, whereas performance declines significantly in the second cycle. The first regeneration retained over 75% efficiency (83.37%), indicating good initial adsorption potential. However, long-term stability remains limited, as the second regeneration showed a sharp decrease to 46.08%. This decline is likely due to irreversible ammonium retention, pore blockage, membrane fouling, zeolite leaching, membrane compaction, or possible acid-induced degradation of cellulose acetate, particularly when HCl is used as the regenerating agent. These findings are consistent with previous studies (Jiang et al., 2024; Pérrez-Botella et al., 2023), which reported that repeated adsorption–desorption cycles lead to performance degradation due to adsorbate retention in smaller or less accessible pores. In addition, the use of concentrated NaCl and HCl may generate secondary waste, which should be considered in future process optimization.

Application of Cellulose Acetate–Zeolite MMMAs in POME Treatment

The performance of cellulose acetate–zeolite mixed matrix membrane adsorbers (MMMAs) for ammonia removal from palm oil mill effluent (POME) was evaluated through batch adsorption and filtration processes. The results are summarized in **Table 9**.

Table 9. Ammonia removal performance for POME samples

Parameter	Regulatory standard (mg/L)	Initial concentration (mg/L)	Adsorption result (*Batch*) (mg/L)	Filtration result (mg/L)
Ammonia	20	173,93	50,161	52,136

As shown in **Table 9**, the initial NH_3-N concentration in Pond 4 was 173.93 mg/L, exceeding the permissible discharge limit of 20 mg/L. After treatment using the cellulose acetate–zeolite MMMAs, both batch adsorption and filtration processes resulted in a substantial reduction in ammonia concentration. The batch adsorption test reduced the NH_3-N concentration to 50.161 mg/L, corresponding to a removal efficiency of 71.16%, while the filtration module reduced the concentration to 52.136 mg/L, with a removal efficiency of 70.02%. The reduction in NH_3-N concentration observed in both batch and filtration tests demonstrates that the membrane effectively reduced ammonia-nitrogen concentration. This performance is attributed to the membrane's dual function as both an adsorption medium and a filtration barrier within a single treatment step.

As the wastewater passes through the membrane, components larger than the membrane pore size, such as suspended and dissolved solids, are retained and prevented from passing through the membrane. Consequently, the permeate obtained is cleaner and contains a lower concentration of contaminants. Based on these findings, it can be concluded that the cellulose acetate–zeolite mixed matrix membrane exhibits strong potential as a pretreatment or polishing component for NH3-N removal in palm oil mill effluent (POME) treatment. However, the treated effluent remained above the regulatory limit of 20 mg/L, indicating that the membrane should not yet be considered a complete standalone treatment and requires further optimization or integration with other treatment methods. The comparison of POME pollutant removal methods used in this study with other methods reported in previous studies is presented in **Table 10**.

In the present study, the batch adsorption/filtration method demonstrated a reduction of NH_3-N from 173.93 mg/L to 50.161 mg/L. While this represents a significant decrease, direct comparison with other POME treatment techniques should be made cautiously because several previous studies

reported total nitrogen rather than ammonia or NH_3-N. Total nitrogen includes organic nitrogen, nitrate, nitrite, and ammoniacal nitrogen, whereas this study focused specifically on NH_3-N. For instance, Yuniarti et al. (2019) utilized the aeration method, which achieved a remarkable reduction in total nitrogen from 91.12 mg/L to just 0.31 mg/L. This shows that aeration is much more efficient in removing total nitrogen compared to batch adsorption/filtration, which focuses primarily on ammonia. In addition, Elystia et al. (2021) used the HRAR (High Rate Alga Reactor) system, which reduced total nitrogen from 408.88 mg/L to 80.28 mg/L.

Table 10. Comparison of POME treatment methods for *ammonia, ammonium, or total nitrogen* removal

No.	Removal Method	Parameter	Initial Value (mg/L)	Final Value (mg/L)	Reference
1.	Aeration method	Total nitrogen	91,12	0,31	Yuniarti et al., 2019
2.	HRAR (*High Rate Alga Reactor*) System	Total nitrogen	408,88	80,28	Elystia et al., 2021
3.	*Constructed Wetland Method*	Nitrogen Ammonium	14,26	1,4	Ujang et al., 2021
4.	Open pond system	Total nitrogen	Not specified	84,798	Vienna et al., 2024
5.	Batch Adsorption/ filtration	NH_3-N	173,93	50,161	This study

This result is better than the batch adsorption/filtration method in terms of total nitrogen removal. The HRAR system relies on microalgae to absorb nitrogen, offering a biologically sustainable approach, though it requires more complex management and longer processing times than the batch method. Similarly, Ujang et al. (2021) reported results using the constructed wetland method, which focused on ammonium removal, reducing ammonium from 14.26 mg/L to 1.4 mg/L. While effective for ammonium removal, this method does not perform as well in reducing total nitrogen compared to aeration or HRAR. Therefore, the present CA-zeolite MMMA should be interpreted as a promising ammonia-nitrogen removal material, but not directly ranked against total-nitrogen removal systems without considering differences in pollutant parameters, initial concentrations, operating conditions, and treatment objectives.

Overall, the results of this study indicate that batch adsorption/filtration is effective for NH3-N removal, but the final concentration remains above the discharge standard. Because aeration and HRAR studies often report total nitrogen, their performance should not be directly compared with the NH3-N removal efficiency of the present membrane system. The choice of method should be based on the specific treatment goals, such as whether ammonia, ammonium, or total nitrogen needs to be addressed. For practical POME treatment, the CA-zeolite MMMA may be more suitable as a pretreatment or polishing unit combined with biological or physicochemical treatment to achieve regulatory compliance.

CONCLUSION

Based on the results of this study, cellulose acetate-zeolite mixed matrix membrane adsorbers (MMMAs) were successfully developed from oil palm empty fruit bunch-derived cellulose acetate and natural mordenite zeolite for ammonia-nitrogen removal from palm oil mill effluent (POME). The incorporation of zeolite improved membrane properties, particularly flux, porosity, and swelling degree, although tensile strength and elongation decreased compared to pristine cellulose acetate membranes. The optimum adsorption performance was achieved at a zeolite loading of 30% and a contact time of 70 minutes, yielding an adsorption capacity of 1.051 mg/g under the selected operating condition. The MMMAs also exhibited satisfactory first-cycle regenerability, with maximum regeneration efficiencies of 83.37% (NaCl) and 73.52% (HCl) in the first cycle. Application to real POME samples resulted in significant ammonia-nitrogen removal, with efficiencies of 71.16%

for batch adsorption and 70.02% for filtration. However, the treated effluent did not meet the regulatory discharge standard, indicating that further process optimization or integration with additional treatment methods is required. A notable limitation is the decline in adsorption performance over successive regeneration cycles, suggesting limited long-term stability. Future work should focus on enhancing membrane durability through material modification, improving zeolite dispersion, optimizing membrane thickness, reducing mechanical-property loss, evaluating lower-impact regeneration agents, and integrating the membrane with biological or physicochemical treatment methods to improve reusability, operational lifespan, and regulatory compliance.

AUTHOR CONTRIBUTIONS

Conceptualization, CR and S; methodology, CR, J, MF, and S; software, CR and J; validation, MF, MRAM, and S; formal analysis, CR and J; investigation, CR, J, and MF; resources, S and MRAM; data curation, CR and J; writing—original draft preparation, CR; writing—review and editing, J, MF, MRAM, and S; visualization, CR and J; supervision, MF, MRAM, and S; project administration, S; funding acquisition, S.

ACKNOWLEDGMENT

This work was fully funded by Universitas Syiah Kuala under the Master's Thesis Research Program. This research was funded by the Ministry of Education, Culture, Research, and Technology of the Republic of Indonesia through the Master's Thesis Research Program under contract No. 113/C3/DT.05.00/PL/2025.

CONFLICTS OF INTEREST

The authors declare no conflict of interest concerning the publication of this article. The authors also confirm that the data and the article are free of plagiarism.

REFERENCES

Aditama, A. G., Farid, M., & Ardhyananta, H. (2017). Isolasi selulosa dari serat tandan kosong kelapa sawit untuk nano fiber komposit absorpsi suara: analisis FTIR. Jurnal Teknik ITS, 6(2). https://doi.org/10.12962/j23373539.v6i2.24098

Amini, A., Aponte-Morales, V., Wang, M., Dilbeck, M., Lahav, O., Zhang, Q., Cunningham, J. A., & Ergas, S. J. (2017). Cost-effective treatment of swine wastes through recovery of energy and nutrients. Waste Management, 69, 508–517. https://doi.org/10.1016/j.wasman.2017.08.009

Amira, A., Sazali, N., & Salleh, W. N. W. (2021). Emerging mixed matrix membranes based on zeolite and cellulose acetate for reverse osmosis applications. Cellulose, 28, 7131–7148. https://doi.org/10.1007/s10570-021-03924-5

Atikah, W.S. (2017). Potensi zeolit alam gunung kidul teraktivasi sebagai media adsorben pewarna tekstil. Arena Tekstil, 32, 17-24. https://doi.org/10.31266/at.v32i1.2650

Aulia, M., Mahmud., & Mu'min, B. (2021). Studi isoterm dan kinetika adsorpsi COD (Chemical Oxygen Demand) pada air sungai terhadap karbon aktif kayu ulin. Jurnal Teknik Lingkungan Universitas Lambung Mangkurat, 2, 23-36. https://doi.org/10.20527/jernih.v4i2.959

Bahmid, N. A., Syamsu, K., & Maddu, A. (2013). Production of cellulose acetate from oil palm empty fruit bunches cellulose. Chemical and Process Engineering Research, 17, 12-26. https://www.iiste.org/Journals/index.php/CPER/article/view/9396/9619

Batu, M. S., Adu, R. E. Y., & Soares, L. P. (2023). Sintesis selulosa asetat dari sabut buah lontar (Borassus flabellifer Linn) dengan variasi volume anhidrida asetat. Hydrogen: Jurnal Kependidikan Kimia, 5, 751-758. https://doi.org/10.33394/hjkk.v11i5.9049

Cozmuta, L. M., Cozmuta, A. M., Peter, A., Nicula, C., Nsimba, E. B., & Tutu, H. (2012). The influence of pH on the adsorption of lead by Na-clinoptilolite: Kinetic and equilibrium studies. Water SA, 38(2), 269–278.

Darmawan, M. T., Muthia, E., & Ihsan, M. (2018). Sintesis dan karakterisasi selulosa asetat dari alfa selulosa tandan kosong kelapa sawit. Jukung Jurnal Teknik Lingkungan, 4, 50-55. https://dx.doi.org/10.20527/jukung.v4i1.4658

Elystia, S., Rizani, V. M., & Muria, S. R. (2021). Penyisihan polutan pada palm oil mill effluent (POME) menggunakan konsorsium mikroalga-bakteri dengan sistem high rate alga reactor (HRAR). Jurnal Sains Teknologi & Lingkungan, 1, 146-159. https://doi.org/10.29303/jstl.v7i1.213

Filho, R. G., Monteiro, D. S., Meireles C. D. S., Assunção, R. M. N., Cerquiera, D. A., & Barud, H. S. (2008). Synthesis and characterization of cellulose acetate produced from recycled newspaper. Carbohyrate Polymers, 73, 74-82. http://dx.doi.org/10.1016/j.carbpol.2007.11.010

Gaol, M. R. L. L., Roganda, S., Yanthi, S., Indra, S., & Renita M. (2013). Pembuatan selulosa asetat dari α-selulosa tandan kosong kelapa sawit. Jurnal Teknik Kimia USU, 2, 33-39. https://doi.org/10.32734/jtk.v2i3.1447

Ginting, D., Duma, T. N., Rahmadani, N., Suryani, Y., Haryanti, R., Fisika, S., Riau, U. M., Kimia, S., & Riau, U. M. (2023). Potensi separator dari selulosa asetat tandan kosong kelapa sawit dan polyvinylidene fluoride untuk aplikasi perangkat penyimpanan energi potential of cellulose acetat separator of empty palm oil fruit. Bunches and Polyvinylidene Fluoride for Energy Storage, 1, 51–59. https://doi.org/10.26418/positron.v13i1.63784

Haafiz, M. K. M., Eichhorn, S. J., Hassan, A., & Jawaid, M. (2013). Isolation and characterization of microcrystalline cellulose from oil palm biomass residu. Carbohydrate Polymer, 93, 628-634. https://doi.org/10.1016/j.carbpol.2013.01.035

Ho, Q. N., Lau, W. J., Jaafar, J., Othman, M. H. D., & Yoshida, N. (2025). Membrane technology for valuable resource recovery from palm oil mill effluent (POME): A review. Membranes, 5, 138. https://doi.org/10.3390/membranes15050138

Jiang, Q., He, J., Wang, Y., Chen, B., Tian, K., Yang, K., Wei, H., Xu, X. (2024). Efficient removal of ammonia-nitrogen in wastewater by zeolite molecular sieves prepared from coal fly ash. Scientific Reports, 14, 21064. https://doi.org.10.1038/s41598-024-72067-x

Lismeri, L., Zari, P. M., Novarani, T., & Darni, Y. (2016). Sintesis selulosa asetat dari limbah batang ubi kayu. Jurnal Rekaya Kimia dan Lingkungan, 82-91. https://doi.org10.23955/rkl.v11i2.5407

Maelan, N. M., Dewi, N. M., Andini, S., Perdani, M. S., & Wahyuningtyas, A. (2024). Adsorpsi logam Cu(II) dengan Hidrogel CMC/Pektin komposisi 2:1 menggunakan metode Freeze-Thaw. KOVALEN: Jurnal Riset Kimia, 2, 126-134. https://doi.org10.22487/kovalen.2024.v10.i2.17273

Marlina, Iqhrammullah, M., Saleha, S., Fathurrahmi, Maulina, F. P., & Idroes, R. (2020). Polyurethane film prepared from ball-milled algal polyol particle and activated carbon

filler for NH_3–N removal. Heliyon, 6(8), e04590. https://doi.org/10.1016/j.heliyon.2020.e04590

Ministry of Environment of the Republic of Indonesia. (2014). Regulation of the Minister of Environment of the Republic of Indonesia Number 5 of 2014 concerning wastewater quality standards. Ministry of Environment of the Republic of Indonesia.

Muttaqi, M. A., David, C. B., Kusno, I., Amin, M., Yusup, H., Amila, D. I., Diego, P. D. (2019). Pengaruh aktivasi secara kimia menggunakan larutan asam dan basa terhadap karakteristik zeolit alam. Jurnal Riset Teknologi Industri, 13, 266-271. https://doi.org/10.26578/jrti.v13i2.5577

Nurman, S., Saiful, Ginting, B., Rahmi, Marlina, & Wibisono, Y. (2021). Synthesis of polyurethane membranes derived from red seaweed biomass for ammonia filtration. Membranes, 11(9), 668. https://doi.org/10.3390/membranes11090668

Nurman, S., Saiful., Rahmi., Ginting, B., & Marlina. (2022). Red seaweed (Gracilaria verrucosa Greville) based polyurethane as adsorptive membrane for ammonia removal in water. Polymers, 14, 1-16. https://doi.org/10.3390/polym14081572

Nuryoto., Naufal, G., Nurmuhammad, R., & Kurniawan, T. (2020). Studi penjerapan amonia menggunakan zeolit alam bayah tanpa aktivasi pada tambak ikan. Jurnal Integritas Proses, 2, 21-26. https://jurnal.untirta.ac.id/index.php/jip/article/download/9172/6615

Ojumu, T. V., Du Plessis, P. W., & Petrik, L. F. (2016). Synthesis of zeolite A from coal fly ash using ultrasonic treatment: A replacement for fusion step. Ultrasonics sonochemistry, 31, 342-349. http://dx.doi.org/10.1007/978-981-16-3937-1-26

Pérrez-Botella, E., Valencia, S., & Rey, F. (2023). Zeolites in adsorption process: State of the art and future prospects. Chemical Review, 24, 17647-17695. https://doi.org/10.1021/acs.chemrev.2c00140

Qadir, D., Mukhtar, H., & Keong, L. K. (2017). Mixed matrix membranes for water purification. Separation & Purification Reviews, 46, 62-80. https://doi.org/10.1080/15422119.2016.1196460

Raja, P. M. (2016). Pemanfaatan membran selulosa asetat termodifikasi mikro zeolit alam untuk filtrasi air sungai. Jurnal Saintika, 2, 37-42. https://jurnal.unimed.ac.id/2012/index.php/lemlit/article/view/12404

Renni C. P., Widhi, M., & Nuni, M. (2018). Pemanfaatan zeolit alam teraktivasi HNO3 sebagai adsorben ion logam Fe(III) dan Cr (VI). Indonesian Journal of Chemical Science, 1, 64-70. https://doi.org/10.15294/ijcs.v7i1.19627

Rohani, R., Yusoff, I. I., Zaman, N.K., Ali, A. M., Rusli, N. A. B., Tajau, R.., & Basiron, S. A. (2021). Ammonia removal from raw water by using adsorptive membrane filtration process. Separation and Purification Technology, 270, 1-8. https://doi.org/10.1016/j.seppur.2021.118757

Rosa, S. M. L., Rehman, N., De Miranda, M. I. G., Nachtigall, S. M., & Bica, C. I. D. 2012). Chlorine-free exctraction of cellulose from rise husk and whisker isolation. Carbohydrate Polymers, 87, 1131-1138. https://doi.org/10.1016/j.carbpol.2011.08.084

Safiah., & Sri, M. (2018). Karakterisasi dan analisa kinerja membran selulosa asetat untuk penyisihan ion logam Cr3+ dan Cd2+ dalam air dengan proses ultrafiltrasi. Jurnal Rekayasa Kimia dan Lingkungan, 2, 127-134. https://doi.org/10.23955/rkl.v13i2.10943

Saiful., Mirzalisa., Raharjo, Y., Widiastuti, N., Wibisono, & Rahmi. (2024). Biomass-based mixed matrix membrane adsorbers for removal of creatinin dialysate fluid. South African Journal of Chemical Engineering, 48, 354-365. https://doi.org/10.1016/j.sajce.2024.03.003

Sanaeepur, H., Nasernejad, B., & Kargari, A., (2015). Cellulose acetate/nano-porous zeolite mixed matrix membrane for CO2 separation. Greenhouse Gases Science and Technology, 3, 291-304. https://doi.org/10.1002/ghg.1478

Septommy, C., & Badriyah, L. (2022). Modifikasi zeolit alam teraktivasi asam dengan perak nitrat. CHEESA, 5, 13-19. https://doi.org/10.25273/cheesa.v5i1.10104.13-19

Setiawan, Y., Mahadmanti, W., & Harjono. (2018). Preparasi dan karakterisasi nanozeolit dari zeolit alam gunungkidul dengan metode top-down. Indonesian Journal of Chemical Science, 1, 43-39. https://doi.org/10.15294/ijcs.v7i1.19074

Sofith, C. D., Effendi, S. R., & Fatimah (2020). Kinerja aktivasi dan impregnasi zeolit alam sebagai adsorben. Jurnal Teknik Kimia USU, 2, 75-79. https://doi.org/10.32734/jtk.v9i2.3764

Ujang, F. A., Roslan, A. M., Osman, N. A., Norman, A., Idris, J., Farid, M. A. A., Halmi, M. I. E., Gozan, M., & Hassan, M. A. (2021). Removal behaviour of residual pollutants from biologically treated palm oil mill effluent by Pennisetum purpureum in constructed wetland. Scientific Reports, 11, 18257. https://doi.org/10.1038/s41598-021-97789-0

Vienna, V., Irhamni., Yunita, I., Zein, I., & Jumali, A. (2024). Efektivitas pengolahan limbah cair pabrik kelapa sawit (PKS) menggunakan sistem kolam terbuka. Karya Ilmiah Fakultas Teknik (KIFT), 2, 6-14. https://ojs.serambimekkah.ac.id/KIFT/article/download/7964/5516

Wang, S., & Peng, Y. (2010). Natural zeolites as effective adsorbents in water and wastewater treatment. Chemical Engineering Journal, 156(1), 11–24. https://doi.org/10.1016/j.cej.2009.10.029

Wibowo, O. V., Martina, A., & Soetedjo, J. N. M. (2018). Penerapan green solvent: ammonium hidroksida pada proses pretreatment cangkang kelapa sawit sebagai adsorben alami dalam pengolahan limbah cair sawit. In Prosiding Seminar Nasional Teknik Kimia (pp. 1-7). Yogyakarta, UPN "Veteran" Yogyakarta. https://jurnal.upnyk.ac.id/index.php/kejuangan/article/view/2259

Yuniarti, D. P., Komala, R., & Aziz, S. (2019). Pengaruh proses aerasi terhadap pengolahan limbah cair pabrik kelapa sawit di PTPN VII secara aerobik. Jurnal Redoks, 2, 7-16. https://doi.org/10.31851/redoks.v4i2.3504

Zhou, L., & Boyd, C. E. (2014). Total ammonia nitrogen removal from aqueous solutions by the natural zeolite, mordenite: A laboratory test and experimental study. Aquaculture, 432, 252–257. https://doi.org/10.1016/j.aquaculture.2014.05.019